OXFORD

International Journal of Neuropsychopharmacology (2019) 22(3): 247–259

doi:10.1093/ijnp/pyy101
Advance Access Publication: January 13, 2018
Regular Research Article

REGULAR RESEARCH ARTICLE

Positive N-Methyl-D-Aspartate Receptor Modulation by Rapastinel Promotes Rapid and Sustained Antidepressant-Like Effects

John E. Donello, Pradeep Banerjee, Yong-Xin Li, Yuan-Xing Guo, BS, Takashi Yoshitake, Xiao-Lei Zhang, Omid Miry, Jan Kehr, Patric K. Stanton, Amanda L. Gross, Jeffery S. Burgdorf, Roger A. Kroes, Joseph R. Moskal

Allergan, Plc, Irvine, California (Dr Donello, Dr Li, Mr Guo); Allergan, Plc, Madison, New Jersey (Dr Banerjee); Department of Physiology and Pharmacology, Karolinska Institutet, Stockholm, Sweden (Drs Yoshitake and Kehr); Department of Cell Biology and Anatomy, New York Medical College, Valhalla, New York (Drs Zhang, Miry, and Stanton); Pronexus Analytical AB, Bromma, Sweden (Dr Kehr); Falk Center for Molecular Therapeutics, Department of Biomedical Engineering, McCormick School of Engineering and Applied Sciences, Northwestern University, Evanston, Illinois (Drs Burgdorf, Kroes and Moskal); Aptinyx, Inc., Evanston, Illinois (Drs Burgdorf, Gross, Kroes and Moskal).

Correspondence: John Donello, PhD, 2525 Dupont Dr., Irvine, CA 92612 (Donello_John@Allergan.com).

Abstract

Background: Modulation of glutamatergic synaptic transmission by N-methyl-D-aspartate receptors can produce rapid and sustained antidepressant effects. Rapastinel (GLYX-13), initially described as a N-methyl-D-aspartate receptor partial glycine site agonist, exhibits rapid antidepressant effect in rodents without the accompanying dissociative effects of N-methyl-D-aspartate receptor antagonists.

Methods: The relationship between rapastinel's in vitro N-methyl-D-aspartate receptor pharmacology and antidepressant efficacy was determined by brain microdialysis and subsequent pharmacological characterization of therapeutic rapastinel concentrations in N-methyl-D-aspartate receptor-specific radioligand displacement, calcium mobilization, and medial prefrontal cortex electrophysiology assays.

Results: Brain rapastinel concentrations of 30 to 100 nM were associated with its antidepressant-like efficacy and enhancement of N-methyl-D-aspartate receptor-dependent neuronal intracellular calcium mobilization. Modulation of N-methyl-D-aspartate receptors by rapastinel was independent of D-serine concentrations, and glycine site antagonists did not block rapastinel's effect. In rat medial prefrontal cortex slices, 100 nM rapastinel increased N-methyl-D-aspartate receptor-mediated excitatory postsynaptic currents and enhanced the magnitude of long-term potentiation without any effect on miniature EPSCs or paired-pulse facilitation responses, indicating postsynaptic action of rapastinel. A critical amino acid within the NR2 subunit was identified as necessary for rapastinel's modulatory effect.

Conclusion: Rapastinel brain concentrations associated with antidepressant-like activity directly enhance medial prefrontal cortex N-methyl-D-aspartate receptor activity and N-methyl-D-aspartate receptor-mediated synaptic plasticity in vitro. At therapeutic concentrations, rapastinel directly enhances N-methyl-D-aspartate receptor activity through a novel site independent of the glycine coagonist site. While both rapastinel and ketamine physically target N-methyl-D-aspartate receptors, the 2 molecules have opposing actions on N-methyl-D-aspartate receptors. Modest positive modulation of

Received: October 8, 2018; **Revised:** December 6, 2018; **Accepted:** December 10, 2018

© The Author(s) 2018. Published by Oxford University Press on behalf of CINP.
This is an Open Access article distributed under the terms of the Creative Commons Attribution Non-Commercial License (http://creativecommons.org/licenses/by-nc/4.0/), which permits non-commercial re-use, distribution, and reproduction in any medium, provided the original work is properly cited. For commercial re-use, please contact journals.permissions@oup.com

Significance Statement

Major depressive disorder (MDD) treatments often take weeks to produce a response, and nearly one-half of all patients fail to adequately respond to treatment. Antagonism of N-methyl-D-aspartate receptors (NMDARs) produces rapid and sustained clinically relevant antidepressant effects, but drugs like ketamine also induce psychotomimetic or dissociative side effects that limit clinical use. Rapastinel, an investigational MDD treatment, was reported to act as a glycine site NMDAR partial agonist, but it was unclear if its antidepressant-like activity was due to enhancement or inhibition of NMDAR activity. Using a variety of techniques, including rodent behavioral testing, microdialysis, calcium imaging, and in vitro and ex vivo electrophysiology, we found that rapastinel brain concentrations that induce antidepressant-like effects directly enhance NMDAR activity and synaptic plasticity via a novel domain independent of the glycine coagonist site. Rapastinel and ketamine have opposite pharmacological effects on NMDAR activity, and rapastinel enhances NMDAR activity to trigger rapid antidepressant-like effects.

N-methyl-D-aspartate receptors by rapastinel represents a novel pharmacological approach to promote well-tolerated, rapid, and sustained improvements in mood disorders.

Keywords: rapastinel, NMDA receptor, depression

Introduction

Major depressive disorder is a burdensome disease that leads to considerable functional impairment. Current antidepressants may take 4 to 8 weeks to achieve full clinical response (Posternak and Zimmerman, 2005), and over 50% of patients experience inadequate response to first treatment (Warden et al., 2007). There is an unmet need for rapid-acting and effective treatments for depressive symptoms.

Glutamatergic neurotransmission and N-methyl-D-aspartate receptors (NMDARs) play important roles in activity-dependent synaptic plasticity, learning, and psychiatric disorders (Skolnick et al., 1996; Wiescholleck and Manahan-Vaughan, 2013; Gerhard et al., 2016). Although research previously concentrated on monoamines, dysfunction in glutamatergic systems is also an important contributor to depression (Sanacora et al., 2012). Antagonism of NMDARs has been suggested to be the pharmacological mechanism by which glutamatergic antagonists (i.e., ketamine) exert rapid and sustained antidepressant effects (Li et al., 2010, 2011; Liu et al., 2012; Niciu et al., 2014; Williams and Schatzberg, 2016). Although it is well established that ketamine, an uncompetitive NMDAR open channel blocker, rapidly relieves depressive symptoms (Berman et al., 2000; Monteggia and Zarate, 2015), clinical studies with other NMDAR antagonists have shown mixed results (Zarate et al., 2006; Sanacora et al., 2017). Recent data also suggest ketamine's rapid antidepressant-like effect may be independent of NMDARs, highlighting the importance of further understanding the pharmacology and efficacy of NMDAR modulation in depression (Zanos et al., 2016; Wohleb et al., 2017; Williams et al., 2018).

Rapastinel (GLYX-13) exerts rapid, sustained antidepressant effects in human clinical trials (Preskorn et al., 2015) and in animal models of depression, including the forced swim test (FST), learned helplessness, novelty-induced hypophagia, chronic unpredictable stress, and social defeat (Burgdorf et al., 2013, 2015a, 2015b; Yang et al., 2016; Liu et al., 2017). Unlike ketamine, rapastinel has been proposed to enhance NMDAR activity by acting as a glycine site functional partial agonist (Moskal et al., 2014), although systematic investigation of its interaction with NMDARs has not been performed. Whole-cell electrophysiological techniques in CA1 pyramidal neurons of rat hippocampal slices demonstrated that rapastinel, in the absence of an NMDAR glycine site agonist, elicits an NMDAR channel current (Moskal et al., 2005, 2014; Zhang et al., 2008) of approximately 20% of the maximum amplitude generated by the NMDAR glycine site full agonist D-serine (Moskal et al., 2014). Low rapastinel concentrations have also been shown to enhance induction of long-term potentiation (LTP) at Schaffer collateral-CA1 synapses (Burgdorf et al., 2013; Moskal et al., 2014). Interestingly, despite potentially opposing effects of rapastinel and ketamine on NMDAR activity, the antidepressant-like effects of rapastinel and ketamine both require AMPA receptor (AMPAR) activation and increased mTORC1 signaling (Maeng et al., 2008; Li et al., 2010; Koike et al., 2011; Burgdorf et al., 2013; Zanos et al., 2016).

The following experiments were designed to characterize rapastinel NMDAR pharmacology and further characterize its antidepressant mechanism of action. Herein, extracellular levels of rapastinel in medial prefrontal cortex (mPFC) at its effective antidepressant doses were assessed to determine if rapastinel's antidepressant efficacy is due to enhancement or inhibition of NMDAR activity. We also examined rapastinel's modulation of recombinantly expressed NMDAR subtypes, isolated cortical neuron NMDAR activity, and native NMDAR ionotropic effects in mPFC tissue slices. Finally, we characterized the impact and concentration-response profile of rapastinel and S-ketamine on LTP formation, a cellular substrate of learning and memory elicited by NMDAR activation (Malenka and Bear, 2004) at mixed excitatory synapses in layer III/IV of the mPFC.

Materials and Methods

Animals

All experiments were approved by the Allergan Institutional Animal Care and Use Committee and carried out in accordance with the Guide for the Care and Use of Laboratory Animals as adopted and promulgated by the US National Institutes of Health.

Drugs

Rapastinel was synthesized in free-base form by Sai Life Sciences (India). S-ketamine was purchased from Sigma-Aldrich (St. Louis, MO). For behavioral and microdialysis studies, rapastinel and S-ketamine were dissolved in sterile saline (0.9% NaCl) and administered s.c. or i.p., respectively.

FST

FST adapted for use in rats was performed as previously described (Burgdorf et al., 2015b). On day 1 (habituation), rats were placed in a transparent cylindrical tube (46 cm tall × 20 cm diameter) filled to 30 cm with water (23°C ± 1°C) for 15 minutes. Water was changed after every other rat; tests were videotaped. Rats were injected with rapastinel (3, 10, or 30 mg/kg, s.c.), S-ketamine (3, 10, or 30 mg/kg, i.p.), or vehicle (sterile saline [1 mL/kg], s.c.) and tested at 60 minutes and 7 days postdose. For testing, rats were placed in the cylindrical tube for 5 minutes and recorded with a computerized video-system Smart 3.0 (Harvard Apparatus). Total time each rat spent immobile, defined as the minimal amount of effort required to keep head above water, was scored by a trained, blinded observer.

Microdialysis

Microdialysis experiments were performed in freely moving rats as previously described (Kehr and Yoshitake, 2006). Guide cannulae were implanted into mPFC at the coordinates: AP, +3.2 mm; L, +0.5 mm; V, –1.5 mm, specified from bregma and the dural brain surface according to the atlas of Paxinos and Watson (2007); the mPFC location was at V –4.5 mm, which was achieved with the length of the microdialysis probe tip. Following 7 days of recovery, a microdialysis probe (3-mm membrane length, 50 kDa cutoff) was inserted into the guide cannula, and mPFC was dialyzed with artificial cerebrospinal fluid (aCSF; flow rate: 1 µL/min) containing (in mM): 148 NaCl, 4 KCl, 0.8 $MgCl_2$, 1.4 $CaCl_2$, 1.2 Na_2HPO_4, and 0.3 NaH_2PO_4 (pH 7.2). Following 3-hour stabilization, samples were collected in 20-minute intervals, 3 at baseline levels and then for an additional 4 hours following drug administration. Rapastinel concentrations were measured by ultra-high performance liquid chromatography tandem mass spectrometry as described previously (Kehr and Yoshitake, 2017).

Target Specificity Assays

Displacement of radioligands by 30 µM S-ketamine, R-ketamine, (R,S)-ketamine, and rapastinel was analyzed in side-by-side experiments from 28 different NMDA and non-NMDAR binding sites. Dose-dependent displacement effects were analyzed in identified targets using a high-throughput electrophysiological system (IonWorks Barracuda system).

[3H] MK-801 Potentiation Assay

Membrane Preparation

Crude membranes were prepared using transiently transfected, human NR2A-D subtype-expressing HEK cells. All procedures were performed at 4°C. Briefly, pelleted cells were washed in 10 mM Tris·acetate (pH 7.4, 4°C), pelleted, and frozen overnight (–80°C). The pellet was resuspended and homogenized (30 strokes) in a glass homogenizer, pelleted at 51 500 × *g* for 30 minutes at 4°C, and stored at –80°C until assay.

Potentiation Assay

Membrane extract protein (300 µg) was preincubated for 15 minutes at 25°C in the presence of saturating concentrations of glutamate (50 µM) and varying concentrations of rapastinel. Following addition of 0.3 mCi of [^{3}H] MK-801 (Amersham, 22.5 Ci/mmol), reactions were incubated for 15 additional minutes (nonequilibrium conditions). Bound and free [^{3}H] MK-801 were separated via rapid filtration. Zero levels were determined in the absence of glycine. Percent maximal [^{3}H] MK-801 binding was calculated relative to stimulation measured in the presence of 1 mM glycine and 50 µM glutamate. Binding curves were fitted using GraphPad.

Neuronal Cultures

Rat brain cortical neurons were obtained from Lonza (R-CX-500; Basel, Switzerland). Cortical cells from embryonic day 18 and 19 were seeded onto poly-D-lysine-coated coverslips and cultured per manufacturer's instructions with slight modifications for cell thawing and culture initiation. Briefly, after removal from liquid nitrogen, cells were heated to 37°C for 2.5 minutes and added to prewarmed medium (Lonza Primary Neuron Basal Medium with 2 mM L-glutamine, 50 µg/mL gentamicin, 37 ng/mL amphotericin, and 2% [v/v] NSF-1) with manual rotation for 2 minutes before being mixed by inversion twice. The cell suspension was plated onto coverslips and incubated for 1 hour (37°C, 5% CO_2). Following incubation, medium containing 10% (v/v) fetal bovine serum (FBS) was added; suspension was further incubated for 3 hours, at which point one-half of the medium was replaced with fresh medium containing 10% FBS. The culture was incubated for 3 to 4 days, and then one-half of the medium was replaced with fresh FBS-free medium. For the next 2 weeks, 500 µL medium was replaced with 1 mL FBS-free medium twice weekly. Cells were used 10 to 28 days following culture initiation.

Intracellular Ca^{2+} Influx Measurement

Dye Loading

Before recording, coverslips containing neuronal culture were removed from the incubator, and medium was removed by washing thrice with extracellular medium (ECM) containing (in mM): 145 NaCl, 5.4 KCl, 10 HEPES, 11 D-glucose, 1.8 $CaCl_2$, 0.000075 TTX, and 0.002 NBQX (pH 7.4). All test compounds were dissolved in ECM. Coverslips were transferred to 35-mm cell culture dishes containing 2.5 mL ECM and 2 µM nonfluorescent acetoxymethyl ester (fluo-4-AM; Molecular Probes, Eugene, OR) and incubated for 25 minutes at room temperature (RT). Cells were washed in ECM and incubated for another 25 minutes to allow complete deesterification of intracellular acetoxymethyl esters.

Optical Recording

Fluo-4-AM loaded cells were continuously perfused at a constant rate of 2 to 3 mL/min with ECM at RT in a recording chamber mounted on an Olympus BX61WI fixed-stage upright microscope equipped with Olympus FluoView confocal imaging system and 20× objective (0.5W). Fluo-4 was excited with an argon laser (488 nm), and digital fluorescence images were captured every 2 seconds. Compounds were applied through a homemade local drug application system with 90% solution exchange time in <1 second.

Data Analysis

Image data were analyzed offline with FV-ASW software (Olympus). Cells were selected based on positive response to maximum stimulation by 10 µM NMDA + 3 µM D-serine. Regions of interest were manually circled around cell bodies; average fluorescence intensities were calculated and plotted for each cell. Data from individual cells were averaged for each coverslip and calculated as mean ± SEM. Fluorescence changes under each condition were calculated by subtracting mean intensity

10 to 30 seconds before drug application from those 10 to 30 seconds after drug application. Change in fluorescence by 10 μM NMDA or NMDA + rapastinel was compared with 10 μM NMDA + 3 μM D-serine, which produced close-to-maximum signal under the current experimental conditions. The raspastinel effect was normalized to the signal induced by NMDA "alone." Cells without significant NMDA "alone" response (<2% maximum) were excluded.

Electrophysiology

Whole-Cell Patch-Clamp Recordings From Cultured Neurons

Whole-cell patch-clamp recordings were conducted in cultured cortical neurons 3 weeks at RT. Glass micropipettes were filled with intracellular solution containing (in mM): 120 Cs-gluconate, 5 NaCl, 10 KCl, 1 EGTA, 2 $MgCl_2$, 10 HEPES, 2 ATP, 10 phosphocreatine, and 0.25 GTP (pH 7.3, 290 mOsm). Ionic currents were measured using an AxoPatch 200B (Molecular Devices, Sunnyvale, CA) filtered at 2 kHz and digitized at 10 kHz. Whole-cell voltage-clamp configuration was established; cells were held at –60 mV or +40 mV. Fast application of NMDA with or without D-serine and/or rapastinel was applied through a homemade local drug application system with 90% solution exchange time in <1 second. Rapastinel was preapplied for 30 seconds before 15 seconds of coapplication of rapastinel + NMDA. Amplitudes of sustained currents were measured as mean current 12 to 14 seconds after agonist application over the 2-second interval.

Preparation of mPFC Slices.

Coronal slices containing mPFC were prepared from 6- to 10-week-old male Sprague-Dawley rats. Rats were deeply anesthetized with isoflurane and decapitated. Brains were rapidly removed and submerged in ice-cold, oxygenated aCSF (2°C–4°C) containing (in mM): 124 NaCl, 2.5 KCl, 2 $CaCl_2$, 2 $MgCl_2$, 1.25 NaH_2PO_4, 26 $NaHCO_3$, and 10 D-glucose (pH 7.4, gassed continuously with 95% O_2/5% CO_2). aCSF was made with deionized, distilled water (resistance >18 MΩ/cm^2; Milli-Q system; Millipore) and salts (Sigma or Fluka). Brains were hemisected, frontal lobes removed, and individual hemispheres glued using cyanoacrylate adhesive to a stage immersed in ice-cold, oxygenated aCSF. Modified coronal slices containing prelimbic and infralimbic regions were cut at 300-μm thickness using Vibratome (Leica VT1200S), as previously described (Parent et al., 2010). Slices were transferred to an interface holding chamber containing oxygenated aCSF for incubation at RT for >1 hour before transferring to a Haas-style interface recording chamber continuously perfused at 3 mL/min with oxygenated aCSF (32°C ± 0.5°C). For all recordings, the bath solution (aCSF) contained (in mM): 125 NaCl, 2.5 KCl, 2 $CaCl_2$, 1 $MgCl_2$, 1.25 NaH_2PO_4, 26 $NaHCO_3$, and 10 dextrose. Picrotoxin (20 μM) was present throughout the experiments to partially reduce inhibitory tone.

Whole-Cell Recordings in mPFC Neurons

Whole-cell patch-clamp recordings from layer II/III mPFC pyramidal neurons were acquired as previously described (Burgdorf et al., 2013). Patch pipette resistance ranged from 6 to 6.5 MΩ when filled with intracellular solution that contained (in mM): 135 $CsMeSO_2$, 8 NaCl, 10 HEPES, 0.2 EGTA, 2 Mg-ATP, 0.3 Na-GTP, and 1 QX-314 (pH 7.25 [adjusted with $Cs(OH)_2$], 275 mOsm). Pyramidal neurons within 80 μm of the slice surface were visualized by infrared differential interference imaging and selected for patching by nonswollen pyramidal shape with a 60× water-immersion objective mounted to a Zeiss microscope (Axioskop 2 FS plus). After whole-cell voltage-clamp configuration was established, access resistance was carefully monitored; only cells with stable access resistance <10% of input resistance that changed <5% over the course of the experiment were included in analyses. Excitatory postsynaptic currents (EPSCs) and spontaneous miniature EPSCs (in 6 mM KCl aCSF) were recorded using MultiClamp 700B (Molecular Devices, Union City, CA), with low-pass filter setting at 1 to 3 kHz. Series resistance was compensated in voltage-clamp mode; patched cells whose series resistance changed by >10% were rejected from analysis. Signals were filtered at 3 kHz and digitized at 10 kHz with a Digidata 1322A controlled by Clampex (v9.2, Molecular Devices). A bipolar tungsten stimulating electrode (FHC, Bowdoin, ME) was placed in mPFC mixed efferent pathways; stimulus pulses (200-μs duration) were delivered at 30-second intervals. Neurons were voltage-clamped at –70 mV to record EPSCs to assess input-output relations and paired-pulse facilitation. Neurons were clamped at –40 mV for recording NMDA currents, to relieve voltage-dependent magnesium block, and slices were perfused with aCSF containing 3 mM calcium, 20 μM picrotoxin, and 10 μM NBQX, to isolate NMDA conductances.

fEPSP and LTP Induction in mPFC Neurons

For extracellular fEPSP recordings, low-resistance recording electrodes were made from thin-walled borosilicate glass (1–2 MΩ after filling with aCSF) and inserted into layers III/IV of the prelimbic region of the mPFC. A bipolar stainless-steel stimulating electrode (FHC Co.) was placed on mixed efferent input pathways in mPFC, which include hippocampal inputs, close to the recording electrode, and constant current stimulus intensity adjusted to evoke approximately half-maximal fEPSPs every 30 seconds (50–100 μA; 100-μs duration). fEPSP slope was measured before and after induction of LTP by linear interpolation from 20% to 80% of maximum negative deflection, and slopes were confirmed as stable to within ±10% for ≥15 minutes before commencing an experiment. Drug treatment started approximately 20 minutes prior to theta burst stimulus trains (TBS). LTP was induced by stimulation of the mixed efferent pathway with 3 high-frequency TBS of 10 × 100 Hz with 5-pulse bursts each, applied at 200-ms inter-burst intervals. Each train was of 2-second duration, and trains were applied 3 minutes apart. Signals were recorded using a differential AC amplifier (A-M Systems, Model 1700) and digitized with an A/D board (1608GX-2AO) using SciWorks (v9.1, DataWave) on an IBM-compatible computer. Data were analyzed initially with Clampfit (v9, Axon Instruments) and further processed with Origin 6.1 (Microcal Software) and CorelDraw 10.0 (Corel). Normalized LTP magnitude was calculated for each slice as ratio of mean slope 47 to 50 minutes following TBS vs 0 to 3 minutes prior to TBS. Dunnett's test or paired *t* test was used for statistical analyses; data are presented as mean ± SEM.

Paired-Pulse Profile Recordings in mPFC

Population compound action potential (population spike, PS) magnitudes were measured as amplitude, defined as vertical distance from negative peak of PS to mean positive peaks on either side. PSs were evoked at a stimulus intensity that elicited 50% maximal amplitude for the first pulse spike. A series of inter-pulse intervals, 10- to 1000-ms duration, was used to study paired-pulse profiles. Four sweeps of PSs were recorded for each inter-pulse interval per slice; responses were averaged. The ratio of the second evoked PS amplitude (PS2) to the first (PS1) was used to determine depression or facilitation, with a ratio >1 corresponding to facilitation and a ratio <1 to depression. Experiments were performed in absence of drug and repeated after 30-minute bath application of 100 nM rapastinel. EPSPs were evoked every 30 seconds during drug application to monitor changes in baseline activity.

Statistical Analysis

Analysis of FST data was performed using Prism 6 statistical software (GraphPad Software); values were calculated as mean ± SEM, and differences were considered to be statistically significant at $P < .05$. The mean basal levels in the control and treated groups were compared by use of 1-way ANOVA followed by Dunnett's multiple comparison test. Paired *t* test (Excel) was implemented for calcium imaging and patch-clamp experiments. Effects of rapastinel on pharmacologically isolated NMDAR-mediated EPSCs, paired-pulse facilitation, and frequency and amplitude of spontaneous miniature EPSCs in mPFC pyramidal neurons were assessed by paired *t* test comparing pre-drug baselines to values in each cell following 20 minutes of drug bath application. Effects of rapastinel on magnitude of LTP in mPFC slices 47 to 50 minutes post-TBS were evaluated by 1-way ANOVA, followed by Fisher's Least Significant Difference test comparing each concentration to the magnitude of LTP in untreated control slices.

Results

Rapastinel Produced Sustained Antidepressant-Like Effects

We first determined the extracellular concentrations of rapastinel in rat mPFC associated with antidepressant-like actions. A single administration of either rapastinel (10 and 30 mg/kg, s.c.) or S-ketamine (10 and 30 mg/kg, i.p.) was sufficient to produce a rapid (within 1 hour) and sustained (>7 days) dose-dependent antidepressant-like effect (Figure 1A). Microdialysis studies in rats revealed that rapastinel rapidly distributed in the brain, with a T_{max} of approximately 20 minutes and a half-life of approximately 20 minutes in extracellular fluid. Minimal and maximal rapastinel antidepressant efficacy was associated with brain concentrations of approximately 30 nM (10 mg/kg) and approximately 100 nM (30 mg/kg), respectively (Figure 1B). Similar concentrations of rapastinel were used in in vitro assays characterizing rapastinel's interaction with NMDAR.

Rapastinel Does Not Bind to NMDAR Glycine Coagonist Site in Radioligand Displacement Assays

Rapastinel did not displace radioligand from any of the known NMDAR ligand sites, including the NMDAR glycine coagonist site, demonstrating that, contrary to previous reports, it does not bind to the NMDAR glycine site. Ketamine stereoisomers significantly displaced radioligand from the NMDAR PCP/MK-801 site (Table 1).

S-ketamine additionally inhibited radioligand binding to opioid receptors (μ and κ opioid receptors) and serotonin transporter (5-HTT) sites, and inhibited α3β4 and α7 nicotinic acetylcholine receptor channel activity (supplementary Tables 1 and 2). In contrast, 30 μM rapastinel did not have a significant effect at any of these sites (supplementary Tables 1 and 2).

Rapastinel Modulates Channel Conformation of NMDARs Containing Any of the Four NR2 Receptor Subtypes A-D

Using membranes derived from HEK cells expressing recombinant human NR1 and NR2 NMDAR subtypes, we assessed the ability of rapastinel to modulate glutamate-induced binding of [^{3}H] MK-801 to the NMDAR channel pore (Urwyler et al., 2009). This assay detects conformational receptor changes, potentially including pregated states that precede ion flux (Erreger et al., 2005). Glycine enhanced [^{3}H] MK-801 binding with an EC_{50} of 100 to 350 nM at NR2A-D subtypes (Figure 2A–D; supplementary Table 3). Compared with glycine, rapastinel partially enhanced [^{3}H] MK-801 binding but with greater potency than glycine (EC_{50} of 9.8 pM, 9.9 nM, 2.2 pM, and 1.7 pM at the NR2A-D subtypes, respectively).

Rapastinel Positively and Negatively Modulates Rat Primary Cortical Neuron NMDAR-Dependent Calcium Flux

Rapastinel modulation of NMDAR-dependent intracellular calcium ($[Ca^{2+}]_i$) mobilization was assessed in rat primary cortical neurons. NMDA and D-serine exhibited EC_{50}s of 2.8 μM and 290 nM, respectively. Bath application of 10 μM NMDA, without

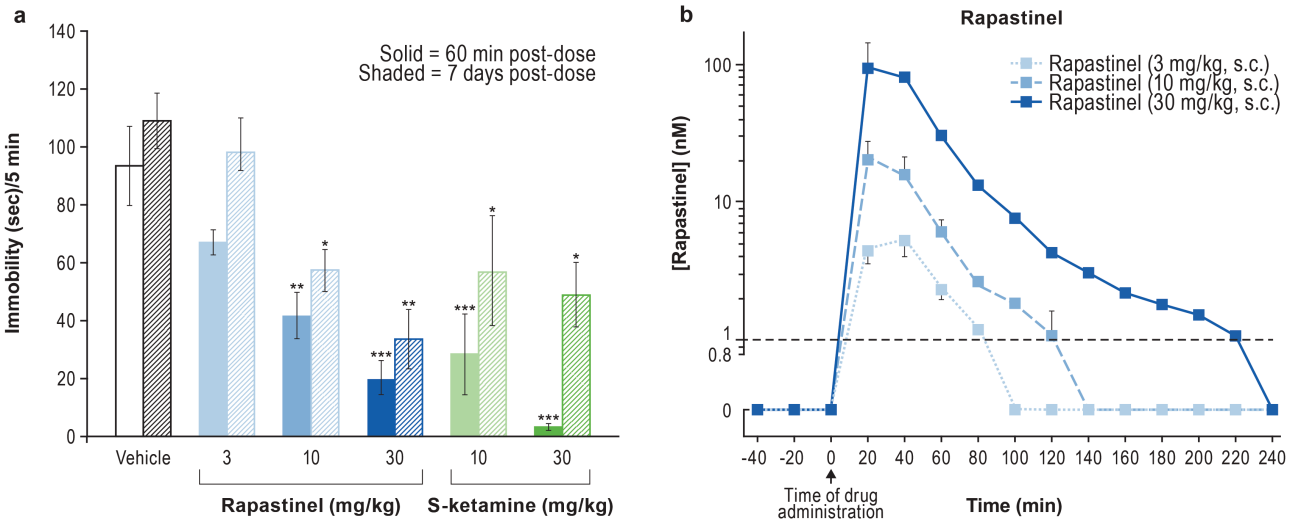

Figure 1. Rapastinel produces an acute and sustained antidepressant-like effect. (A) Rapastinel and S-ketamine produce dose-dependent antidepressant-like responses in the rat forced swim test (FST; n = 6 rats per group, $^*P < .05$, $^{**}P < .01$, $^{***}P < .001$ vs vehicle, 1-way ANOVA, Bonferroni's multiple comparison test). (B) Dose-dependent increase in extracellular levels of rapastinel in medial prefrontal cortex (mPFC) of awake rats (n = 3 rats). Dashed line indicates lower limit of quantitation. Data are mean ± SEM.

Table 1. Ketamine, But Not Rapastinel, Displaces Radioligand from NMDAR Binding Sites

Assay	30 μM S-ketamine	30 μM R-ketamine	30 μM (R,S)-ketamine	30 μM Rapastinel
NMDA, MK-801(%)	**98**	**89**	**96**	2
NMDA, PCP (%)	**84**	**88**	**94**	–7
NMDA, polyamine (%)	–17	1	–16	8
NMDA, glutamate (%)	–6	6	–5	1
NMDA, glycine (%)	0	–5	17	8

Radioligand displacement at NMDAR binding sites by 30 μM S-, R-, and (R,S)-ketamine and rapastinel was analyzed in side-by-side experiments. All ketamine isomers showed meaningful inhibition at the MK-801 and PCP NMDA sites, whereas rapastinel did not show any affinity for any tested NMDAR binding sites. Results which show an inhibition greater than 50% (numbers in bold) are considered to represent meaningful inhibition of the test compound.

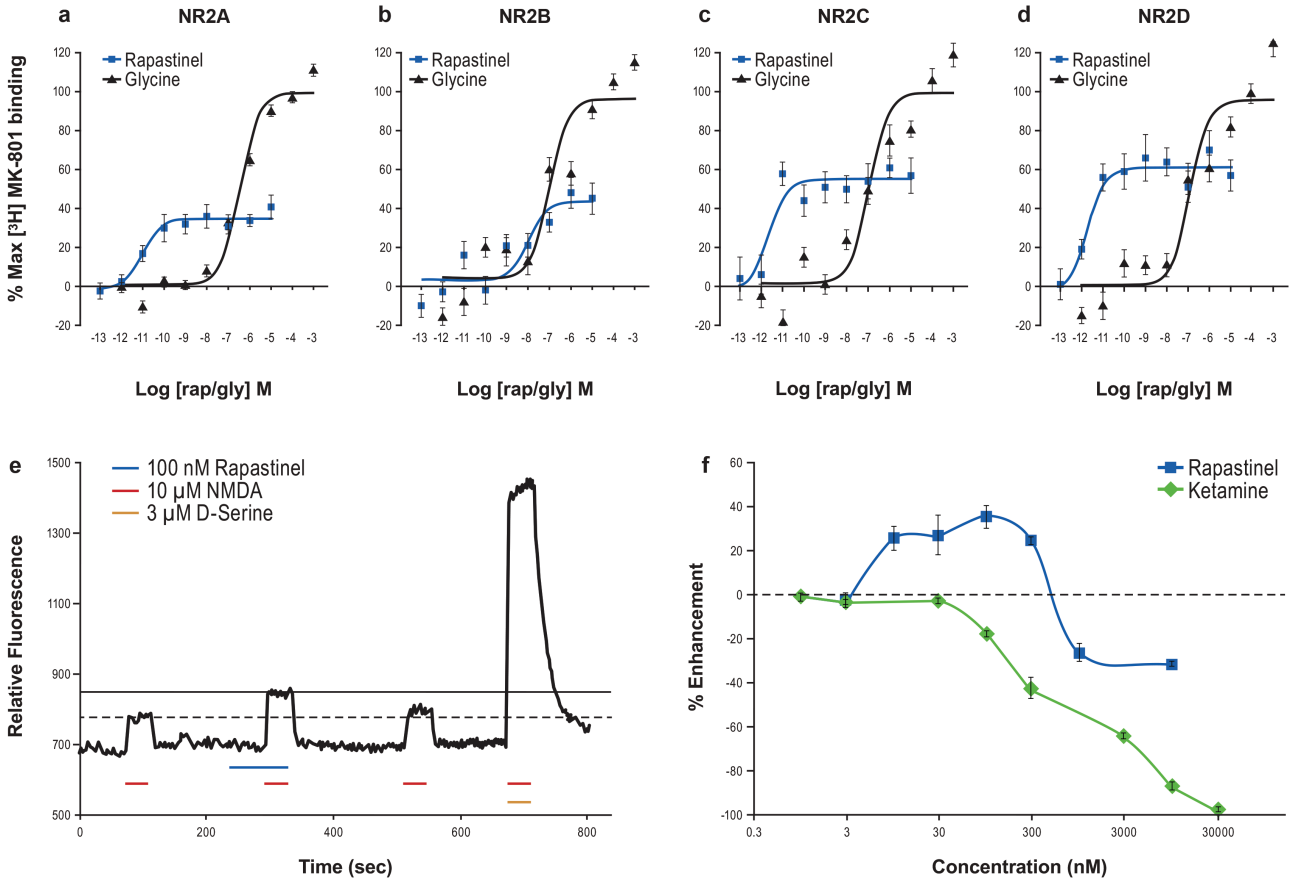

Figure 2. Rapastinel enhances N-methyl-D-aspartate receptor (NMDAR) function in NMDAR subtype-expressing HEK and cultured rat cortical neurons. (A–D) Rapastinel enhances [^{3}H] MK-801 binding in HEK cells expressing NR2A (A; n = 25 glycine, n = 7 rapastinel), NR2B (B; n = 25 glycine, n = 11 rapastinel), NR2C (C; n = 14 glycine, n = 8 rapastinel), and NR2D (D; n = 13 glycine, n = 8 rapastinel). (E) Rapastinel enhances the NMDA-induced intracellular calcium ($[Ca^{2+}]_i$) increase in primary rat cortical neurons. The NMDAR-dependent functional impact of rapastinel and S-ketamine was determined by sequentially infusing cortical neurons with 10 μM NMDA, 10 μM NMDA + rapastinel (or S-ketamine), 10 μM NMDA, and 10 μM NMDA + 3 μM D-serine. (F) Enhancement and inhibition of 10 μM NMDA-induced $[Ca^{2+}]_i$ increase is concentration specific with rapastinel (n = 3–8), whereas S-ketamine blocks the response in a concentration-dependent fashion (n = 4–8). Data are mean ± SEM.

exogenous D-serine, promoted a small, reproducible increase in $[Ca^{2+}]_i$ as measured by an increase in fluo-4 fluorescence (Figure 2E). S-ketamine fully inhibited NMDAR-mediated $[Ca^{2+}]_i$ accumulation in a concentration-dependent manner with an IC_{50} approximately 1.0 μM (Figure 2F). Application of rapastinel (all tested concentrations) in the absence of NMDA had no effect on baseline NMDAR activity or Ca^{2+} fluorescence. However, in the presence of 10 μM NMDA, 10 to 300 nM rapastinel enhanced NMDA-induced Ca^{2+} influx by approximately 30%, whereas concentrations ≥1 μM partially inhibited (approximately 25%) NMDAR activity (Figure 2E–F). The potentiation effect of 100 nM rapastinel on NMDA-induced current was analyzed in cultured cortical neurons under whole-cell patch-clamp recordings (Figure 3). NMDAR-mediated currents were recorded at –60 mV or +40 mV in Mg^{2+}-free solution. As shown in Figure 3B, rapastinel's effect is independent on the membrane potential. In the presence of 0.8 mM Mg^{2+}, NMDA-induced currents were able to be recorded when the membrane potentials were held at +40 mV. Under this relevant physiological condition, rapastinel significantly enhanced NMDAR current (Figure 3C).

Rapastinel-Enhancing Activity Requires NMDA/Glutamate and Is Independent of D-Serine Concentration

We evaluated whether rapastinel's effects on NMDAR were dependent on NMDAR ligand by varying NMDA and D-serine concentration. In the presence of 10 μM NMDA, 100 nM

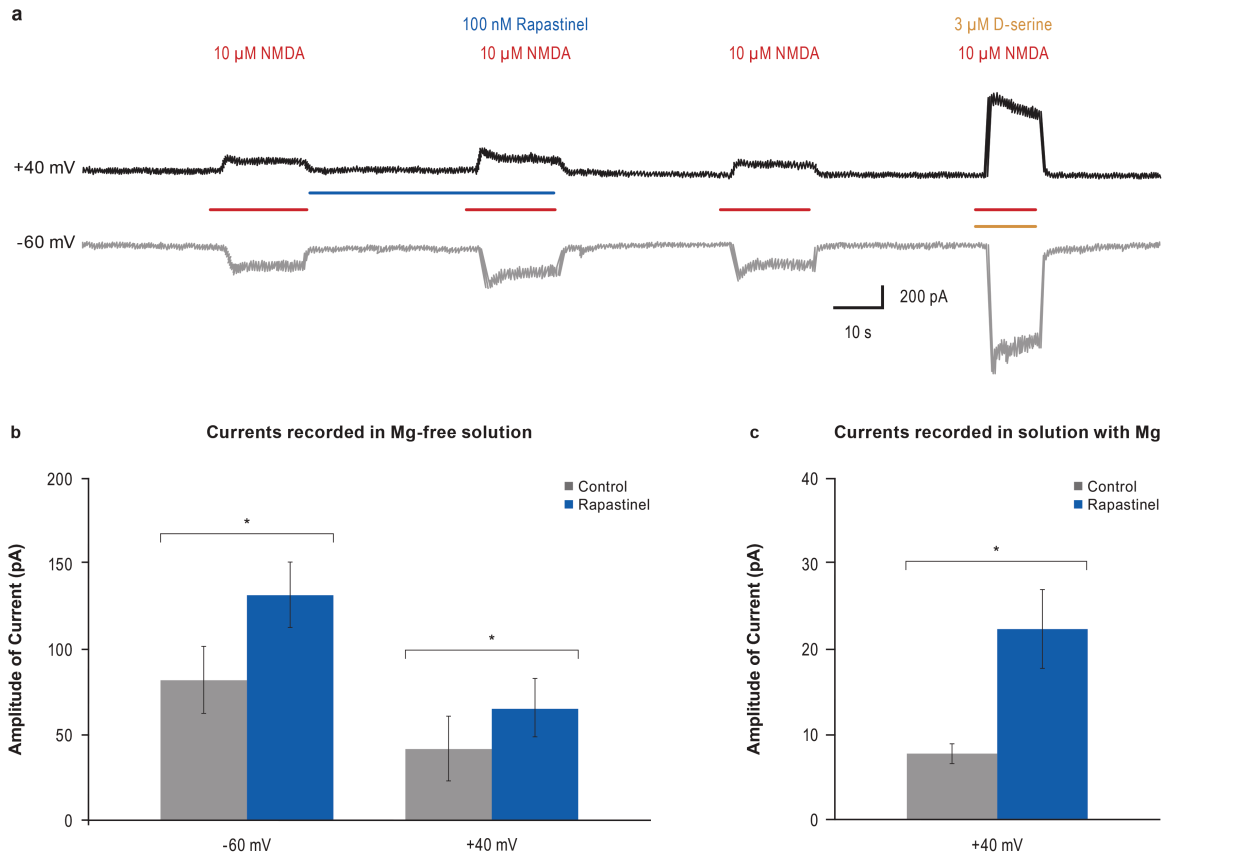

Figure 3. Enhancement of *N*-methyl-D-aspartate receptor (NMDA)-activated currents by 100 nM rapastinel with or without magnesium. (A) Representative traces from cultured cortical neurons voltage-clamped at +40 mV or at –60 mV. (B) Quantification of current amplitude in A (Vm –60 mV: n = 7; Vm +40 mV: n = 3, *P < .05, paired *t* test). NMDA current amplitudes measured in magnesium-free solution were increased at both –60 mV and +40 mV following application of 100 nM rapastinel. (C) With magnesium, NMDA current amplitudes were increased following application of 100 nM rapastinel when held at +40 mV (n = 5, P = .03). Data are mean ± SEM.

rapastinel induced a modest, constant enhancement of NMDA-induced calcium response, irrespective of increasing D-serine concentrations. However, 100 nM rapastinel did not enhance maximum NMDAR activity stimulated by 10 μM NMDA + 3 μM D-serine (Figure 4A). In the presence of 3 μM D-serine, 100 nM rapastinel also enhanced NMDA-induced calcium response at submaximal NMDA concentrations (3–5 μM) (Figure 4B). In contrast, increasing either D-serine or NMDA concentrations had little impact on the inhibitory effect of 1 μM rapastinel (Figure 4C–D). The concentration-specific potentiation/inhibition profile of rapastinel was similar in cortical neurons and HEK cells heterologously expressing NR2A/NR1 or NR2B/NR1 NMDAR (Figure 4E), stimulated with 3 μM NMDA + 3 μM D-serine or 100 nM glutamate + 3 μM D-serine, respectively. Low concentrations of rapastinel (30–100 nM) enhanced NMDAR-induced calcium responses, whereas ≥1 μM rapastinel weakly inhibited these responses (Figure 4E). Rapastinel's inhibitory activity was independent of agonist or coagonist concentrations.

NMDAR Activity Is Modulated by Rapastinel in the Presence of the Competitive Glycine Site Antagonists 7-Chlorokynurenic Acid or MDL 105,519

The compounds 7-chlorokynurenic acid (7-CK) and MDL 105,519 (MDL) are potent glycine coagonist site NMDAR antagonists. Radioligand binding experiments showed that 7-CK had an IC_{50} of 0.56 μM at the strychnine-insensitive [^{3}H] glycine binding site, and 100 μM 7-CK completely blocked NMDAR current in rat cortical slices (Kemp et al., 1988). MDL is significantly more potent and completely inhibited the binding of [^{3}H] glycine to rat brain membranes with a K_i of 10.9 nM (Baron et al., 1997). In the cultured cortical neuron calcium assay, 300 μM 7-CK or 10 μM MDL completely abolished 10 μM NMDA-induced calcium response (Figure 4F–G); this also suggests that nonsaturating levels of endogenous coagonist existed within the assay. Importantly, 10 μM MDL also blocked (–98.5 ± 0.2%, n = 5) the activation of NMDARs by 10 μM NMDA and 100 μM D-serine. Thus, 300 μM 7-CK or 10 μM MDL is at an excess, saturating concentration, which fully antagonized the glycine coagonist site. Saturating concentrations of glycine antagonists, even without addition of exogenous D-serine, did not antagonize the activity of 100 nM rapastinel (Figure 4G). Although 300 μM 7-CK or 10 μM MDL abolished the activity of 10 μM NMDA, additional co-infusion of 100 nM rapastinel restored activity, as evidenced by a small $[Ca^{2+}]_i$ increase similar in magnitude to the overall enhancement induced by rapastinel in other conditions (Figure 4F–G). Furthermore, co-infusion of 100 μM (2*R*)-amino-5-phosphonopentanoate—a competitive glutamate binding site NMDAR antagonist—inhibited the calcium response (Figure 4F–G), suggesting that rapastinel's effect is NMDAR mediated but independent of the glycine coagonist site. This is further confirmed by [^{3}H] MK-801 binding at mutant NR1-NR2B receptors with NR1 subunits containing a loss-of-function mutation in the glycine binding site (F484A/T518L). Whereas glycine failed to enhance [^{3}H] MK-801 binding at mutant receptors (Figure 5A), rapastinel enhanced [^{3}H] MK-801 binding equally in cells expressing wild-type or mutant NR1 subunits (Figure 5B).

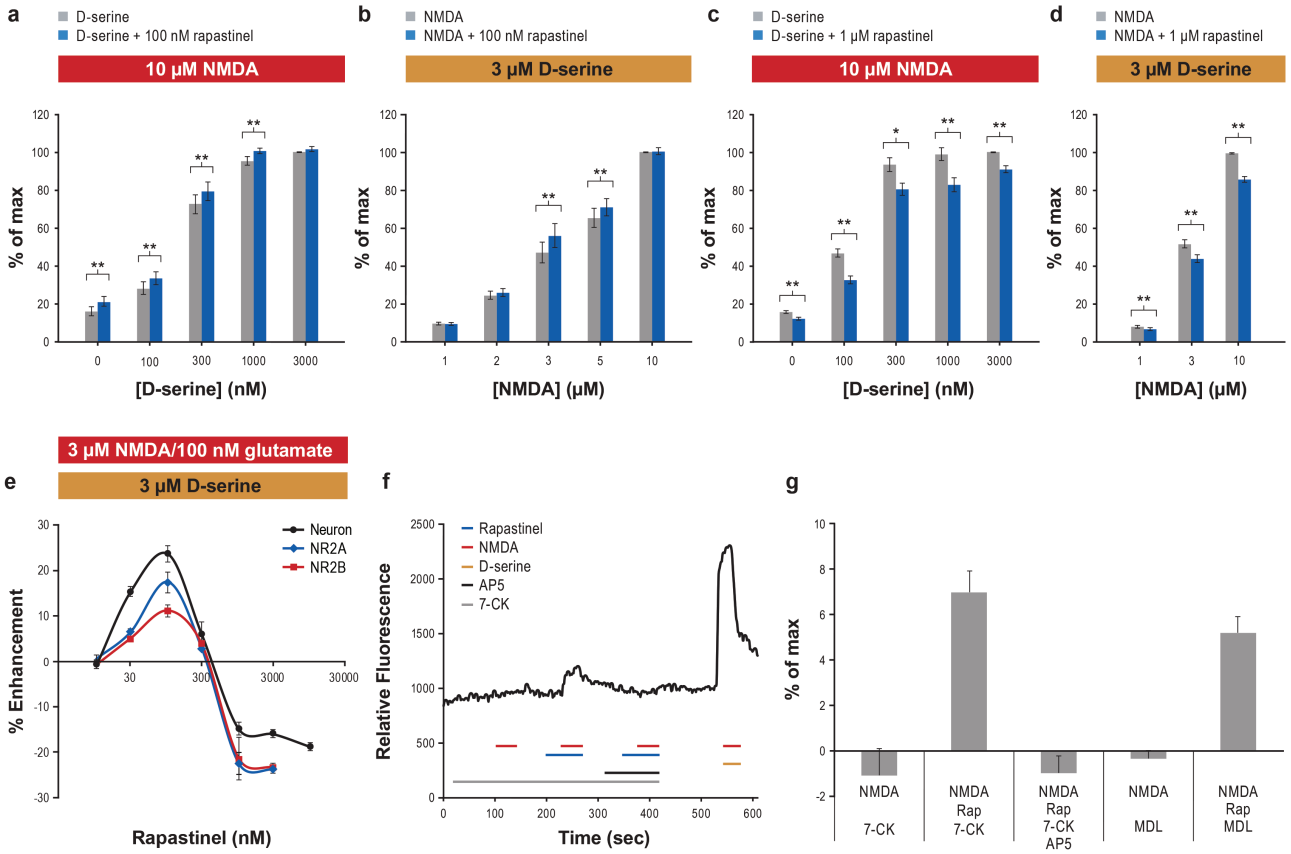

Figure 4. Rapastinel acts independent of the glycine coagonist site as a weak *N*-methyl-D-aspartate receptor (NMDA) coagonist or inhibitor. (A–D) The effect of 100 nM (A–B) and 1 μM (C–D) rapastinel on NMDA-induced calcium response in the presence of 10 μM NMDA and varying concentrations of D-serine (A,C; n = 5–10, *P < .05, **P < .01, paired *t* test), and 3 μM D-serine and varying concentrations of NMDA (B,D; n = 8–13, **P < .01, paired *t* test). Data are normalized to 10 μM NMDA+3 μM D-serine, which is considered maximum response (100%). (E) Dose-dependent effect of rapastinel on $[Ca^{2+}]_i$ changes elicited by 3 μM NMDA+3 μM D-serine in cortical neurons or by 100 nM glutamate+3 μM D-serine in NR2A- or NR2B-expressing HEK cells (n = 5–12). (F) Representative trace of NMDA (10 μM)-induced calcium response with 100 nM rapastinel in the presence of 300 μM 7-CK with or without 100 μM (2R)-amino-5-phosphonopentanoate. (G) Rapastinel (100 nM)'s effect on NMDA (10 μM)-induced calcium response is not abolished by 300 μM 7-CK or 10 μM MDL 105,519 (n = 5–12, *P* < .01 paired *t* test for NMDA+rapastinel+7-CK vs NMDA+7-CK or for NMDA+rapastinel+MDL vs NMDA+MDL) but is completely blocked by (2R)-amino-5-phosphonopentanoate. Data are mean ± SEM.

Potential Effective Site of Rapastinel

Molecular modeling in silico identified a potential high-affinity rapastinel binding site within the amino terminal domain. Point mutagenesis of critical amino acids within the predicted binding domain (R392E in NR2A and analogous R393E in NR2B) did not significantly alter the pharmacological activity of glutamate or D-serine. For the NR2A receptor, 3 μM D-serine and 100 nM glutamate activated the wild-type receptor (32.8 ± 3.5% of 1 μM glutamate; n = 13), and the mutant NR2A (R392E) was not significantly different (29.4 ± 3.0%; n = 16; *P* = .46 vs wild-type NR2A, Student's *t* test). For the NR2B receptor, 100 nM glutamate also activated both the wild-type (22.3 ± 2.6%; n = 14) and mutated (R393E) receptor (22.6 ± 1.2%; n = 19; *P* = .92 vs wild-type NR2B, Student *t* test). Despite the similar response of mutated receptors to glutamate and D-serine, the point mutation in both receptor subtypes completely abolished the potentiation and inhibition of glutamate-induced intracellular calcium mobilization by 100 nM and 1 μM rapastinel, respectively.

Rapastinel Enhances NMDAR-Mediated EPSCs in Rat Pyramidal Neurons in mPFC Slices

Using whole-cell patch clamp recording, exposure to 100 nM rapastinel enhanced NMDAR-dependent EPSCs in mPFC pyramidal neurons without altering current kinetics (Figure 6A), presynaptic glutamate release assessed by paired-pulse response (Figure 6B), or spontaneous miniature EPSC frequency or amplitude (Figure 6C).

Rapastinel, but Not S-Ketamine, Potentiates the Induction of NMDAR-Dependent LTP

Bath application of increasing concentrations of rapastinel 20 minutes prior to TBS produced a biphasic enhancement of the magnitude of LTP. Low rapastinel concentrations significantly increased the magnitude of LTP, with maximal effect observed at 100 nM, whereas high rapastinel concentrations (1 μM) reduced LTP magnitude (Figure 6D–E). In contrast, increasing concentrations of S-ketamine dose-dependently inhibited LTP formation at all concentrations tested, with complete blockade observed at 3 μM (Figure 6E).

Discussion

Rapastinel has been established as an important new compound in psychiatry. It is a positive NMDAR modulator that has been shown to produce rapid-acting and long-lasting antidepressant effects, with a lower propensity than ketamine to induce dissociative and psychotomimetic side effects (Preskorn et al., 2015). Significant acute effects on obsessions and compulsions were also seen in a recent obsessive-compulsive clinical trial (Rodriguez et al., 2016). This study reveals that rapastinel has a

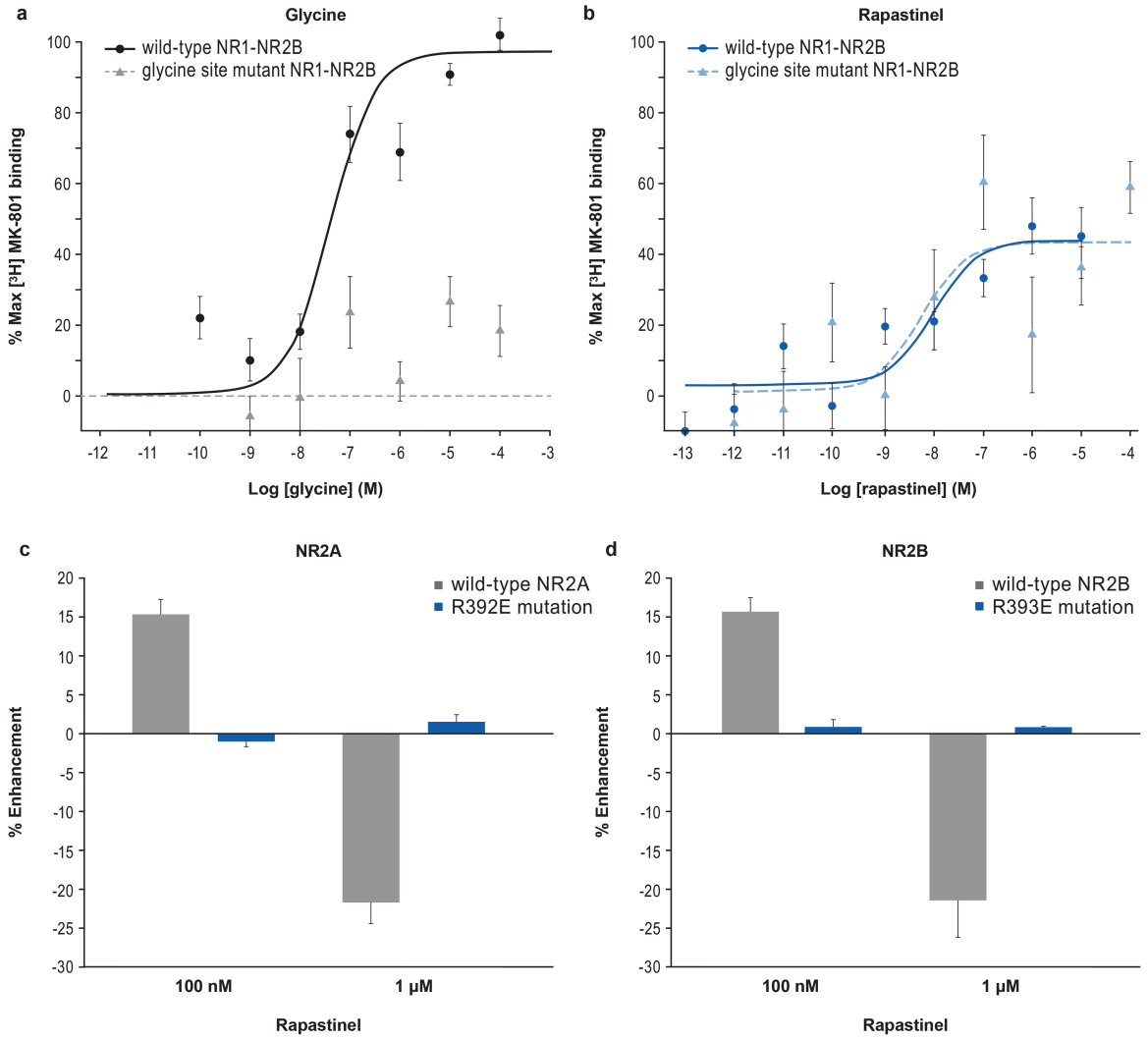

Figure 5. Rapastinel functional site is different from the glycine binding site. (A) Glycine increased [^{3}H] MK-801 binding in wild-type NR1-NR2B controls but not in NR1-NR2B-expressing HEK cells containing a loss of function mutation in the glycine binding site (F484A/T518L) (n = 18). (B) Rapastinel increased [^{3}H] MK-801 binding in both wild-type and glycine mutant cells (n = 18, 2-tailed *t* test). The modulation of *N*-methyl-D-aspartate receptor (NMDA)-induced intracellular calcium response of rapastinel was abolished in HEK293 cells transiently transfected with a (C) R392E mutation in NR2A and (D) R393E mutation in NR2B. Data are mean ± SEM.

novel mechanism of action, which mediates its antidepressant actions; thus, a novel target site and mechanism of glutamatergic modulation may exist for the treatment of mood disorders.

The data herein demonstrate that rapastinel modulates NMDARs directly and can enhance or decrease receptor activity via a novel pharmacological mechanism. Rapastinel does not require glycine or the glycine binding site to enable glutamate-induced receptor activation, demonstrating that it is a coagonist with glutamate rather than a functional glycine site partial agonist as previously thought (Zhang et al., 2008; Burgdorf et al., 2013; Moskal et al., 2014; Preskorn et al., 2015). Our data show that maximal modulation of receptor, either activation or inhibition, is in the range of 20% of the maximum possible activation/inhibition of the receptor (Figure 2F). Although further experimentation is required to fully characterize the rapastinel binding site, initial evidence suggests that this modulation occurs through its potential interaction at a unique binding domain near the amino terminal-ligand binding interface of the receptor. Thus, the potent but modest positive modulation of NMDARs by rapastinel represents a unique therapeutic profile that is effective, well tolerated (Preskorn et al., 2015; Rodriguez et al., 2016), and sufficient to treat CNS disorders associated with diminished glutamatergic tone or synaptic strength with minimal or no negative side effects.

Recently, there have been several NMDAR antagonists (eg, ifenprodil, ketamine, and S-ketamine) and one partial agonist (D-cycloserine) tested in depression clinical trials. Of these, ketamine has been the most thoroughly studied. Based on ketamine's rapid-acting and long-lasting antidepressant effects, coupled with its NMDAR channel-blocking properties, the prevailing idea has been that NMDAR antagonism is how an effective glutamatergic modulator must work to be antidepressant. Using ketamine as a comparator, there are several noteworthy observations to be made. First, the idea that ketamine's antidepressant actions are due to direct NMDAR inhibition is still being investigated. Miller et al. (2016) suggested that both rapid and sustained antidepressant effects of ketamine are dependent on a presynaptic surge of glutamate release triggered by GABAergic interneuron disinhibition, which, in turn, activates pyramidal cell AMPARs. In contrast to ketamine, rapastinel does not affect presynaptic glutamate release as assessed by paired-pulse response and miniature EPSC frequency. Zanos et al. (2016) reported that ketamine's

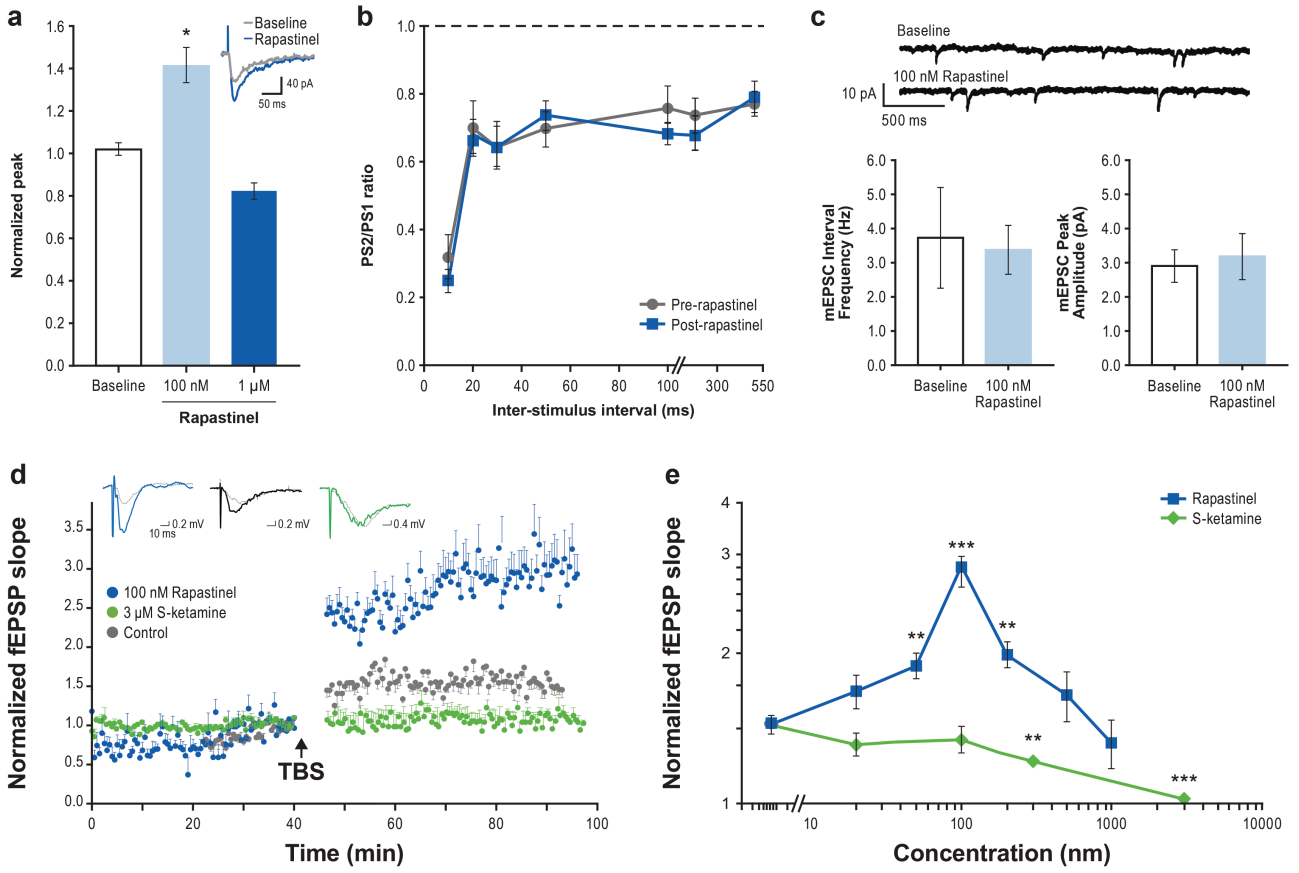

Figure 6. Rapastinel potentiates N-methyl-D-aspartate receptor (NMDAR)-mediated excitatory postsynaptic currents (EPSCs) and acutely enhances long-term potentiation (LTP) in medial prefrontal cortex (mPFC) pyramidal neurons. (A–C) Increase in the amplitude of pharmacologically-isolated NMDAR-mediated EPSCs with 100 nM or 1 μM rapastinel (A; n = 6, $P < .05$, paired *t* test) with no change in NMDAR current kinetics (inset), paired-pulse response profiles in the mPFC measured as ratio of the second population spike response to the first (PS2/PS1) (B: n = 9, $P > .20$, paired *t* test), or frequency or amplitude of spontaneous miniature EPSCs recorded in mPFC pyramidal neurons (C; n = 6, $P > .20$, paired *t* test). (D) Enhancement of the magnitude of LTP induction in mPFC slices by theta burst stimulus trains (TBS) and treated with 100 nM rapastinel starting 20 minutes prior to TBS (n = 8, $P < .01$, Fisher's least significant difference [LSD] test; fEPSP, field excitatory postsynaptic currents) compared with slices treated with 3 μM S-ketamine (n = 7) and untreated control slices (n = 8). Inserts are representative signal averages of 4 fEPSPs before (dotted grey) and 47 to 50 minutes after TBS with 100 nM rapastinel (blue), control (black), or 3 μM S-ketamine (green). (E) Effects of varying concentrations of rapastinel and S-ketamine on LTP of excitatory postsynaptic potentials (n = 6–9 slices, $^{**}P < .01$, $^{***}P < .001$ vs untreated control slice LTP, Fisher's LSD test). Data are mean ± SEM.

antidepressant properties are due to its metabolite(s), which is the agent that actually activates AMPAR activity. Rajagopal et al. (2016) have reported that rapastinel rescues ketamine-induced declarative memory deficits in mice. Clearly, ketamine is working by a different mechanism than rapastinel. Since the psychotomimetic and rewarding effects of ketamine are linked to surges of glutamate and dopamine efflux, respectively (Moghaddam et al., 1997; Lorrain et al., 2003; Valentine et al., 2011; Abdallah et al., 2015), our data suggest that the absence of psychotomimetic-like effects with rapastinel is likely due to its lack of effect on presynaptic glutamate release. Most importantly, rapastinel concentrations sufficient to enhance mPFC NMDAR activity and mPFC synaptic plasticity in vitro are sufficient to trigger antidepressant-like activity in vivo. Taken together, these data suggest that rapastinel's rapid antidepressant-like activity is initiated by a direct postsynaptic enhancement of NMDAR-gated conductance that persistently enhances the magnitude of NMDAR-mediated synaptic plasticity at excitatory synapses in the mPFC. This is consistent with previous work that demonstrated rapastinel's antidepressant activity was blocked by the NMDAR antagonist CPP (Burgdorf et al., 2015b).

To understand rapastinel's in vivo mechanism of action, mPFC concentrations associated with efficacy and its impact on target cell NMDAR function must be characterized. Focal infusion of rapastinel in the mPFC induces antidepressant-like effects (Burgdorf et al., 2013), and rapastinel exhibits a similar dose response across a wide range of depression models. Rapastinel mPFC concentrations of 30–100 nM were sufficient to induce rapid and long-lasting antidepressant-like response. In vitro, 100 nM rapastinel was sufficient to significantly enhance mPFC isolated neuron NMDAR-dependent calcium mobilization, mPFC pyramidal cell peak NMDAR current, and mPFC LTP. Previous studies have focused upon hippocampal CA1 neurons and the electrophysiological effect of 1 μM rapastinel, reporting that 1 μM rapastinel reduced peak NMDAR current, spontaneous inhibitory postsynaptic currents, and spontaneous EPSCs in these neurons (Zhang et al., 2008; Widman and McMahon, 2018). However, we find that lower, efficacious concentrations of rapastinel (30–100 nM) had the opposite effect as it directly enhanced NMDAR activity and mPFC synaptic plasticity. Rapastinel exhibits an unusual inverted U-dose response on recombinantly expressed NMDARs, mPFC NMDAR current, hippocampal and mPFC LTP, animal models of depression, and a human depression clinical trial. A notable exception was the MK-801 accumulation assay, which did not exhibit this same U-shaped dose response; however, the MK-801 assay is

a nonequilibrium assay that detects NMDAR conformational changes, which then allows MK-801 access to the channel pore, and it is unclear how the conformational changes relate to activation or inactivation of NMDAR ionotropic activity. Given rapastinel does not compete for the natural ligand agonist or co-agonist site, further in-depth investigation of the rapastinel's modulatory action is necessary to understand the mechanism by which high concentrations of rapastinel weakly inhibit NMDARs. This general U-shaped dose response raises an interesting possibility that higher peak drug concentrations, which weakly inhibit NMDARs, may be less effective or even counteract the effect of lower concentrations that directly enhance NMDAR function. Regardless, the novel findings that rapastinel is more potent in the mPFC and the elucidation of the efficacious mPFC concentrations has clarified that rapastinel likely evokes antidepressant-like activity by direct enhancement of NMDAR-triggered synaptic plasticity.

In addition to inducing long-lasting changes in synaptic strength, altering NMDAR activity can shift the threshold for induction of future activity-dependent synaptic plasticity, phenomena referred to as "metaplasticity," which come in a variety of related forms and mechanisms (Vose and Stanton, 2017). Both ketamine and rapastinel administered in vivo can elicit metaplastic shifts that result in larger LTP, and this enhancement in LTP appears to be required for antidepressant activity outlasting drug presence (Burgdorf et al., 2013; Izumi and Zorumski, 2014). These data suggest that either blocking or enhancing NMDAR activity can activate long-lasting metaplasticity that promotes induction of LTP-mediating persistent antidepressant actions.

Through a variety of techniques, this study sought to more fully describe the in vitro and in vivo NMDAR pharmacology of rapastinel. The measurement of NMDAR-dependent intracellular calcium accumulation has proven to be a critical assay to identify and characterize rapastinel's modest NMDAR modulatory effect. Although highly reproducible and sensitive, the calcium imaging is an amplified assay with a limited linear range; however, these properties are ideal for identifying and characterizing a modest modulatory effect. Given this moderate effect, it will be difficult but important for future studies to extend rapastinel's dose response and ligand dependence with an electrophysiological study of rapastinel's modulatory effect on current of recombinantly-expressed NMDARs.

In conclusion, positive modulation of NMDARs by rapastinel exhibits rapid and long-lasting antidepressant properties with a lower propensity than ketamine to induce dissociative and psychotomimetic side effects. Rapastinel's mechanism of action is unique and involves NMDAR activation via binding to a novel domain. Receptor activation occurs in the absence of glycine; pharmacologically, rapastinel is a weak modulator that enhances NMDAR activity at antidepressant-like concentrations and inhibits NMDAR activity at higher concentrations. We show here that rapastinel is mechanistically distinct from NMDAR antagonists that also show antidepressant properties. Thus, rapastinel not only has therapeutic potential as an antidepressant but also reveals a novel component of the mechanistic underpinnings of glutamatergic modulation of psychiatric disorders resulting from enhancement of NMDAR activation.

Supplementary Materials

Supplementary data are available at International Journal of Neuropsychopharmacology (IJNPPY) online.

Funding

These studies were supported by funding from Allergan (Madison, NJ, Grant number 10.13039/100007819).

Acknowledgments

The authors thank Chau Vu for preparing and maintaining all cortical neurons used in calcium imaging experiments, Fu-Hua Wang for performing forced swim test experiments, Fumio Ichinose for performing microdialysis experiments, Staffan Schmidt for carrying out LC-MS/MS analysis of microdialysis samples, and Linnea Vose and Alexander Moghadam for performing and analyzing data from extracellular recordings in cortical slices. Writing and editorial assistance was provided by Krystina Neuman, PhD, of Prescott Medical Communications Group (Chicago, IL), a contractor of Allergan.

Interest Statement

J.E. Donello, P. Banerjee, Y.-X. Li, and Y. Guo are employees of Allergan. T. Yoshitake and J. Kehr are affiliated at Karolinska Institutet. J. Kehr is an employee of Pronexus Analytical AB, whose research was funded by Allergan. A.L. Gross, J.S. Burgdorf, R.A. Kroes, and J.R. Moskal are employees of Aptinyx. X.-L. Zhang, O. Miry, and P.K. Stanton have nothing to disclose.

References

Abdallah CG, Sanacora G, Duman RS, Krystal JH (2015) Ketamine and rapid-acting antidepressants: a window into a new neurobiology for mood disorder therapeutics. Annu Rev Med 66:509–523.

Baron BM, Harrison BL, Kehne JH, Schmidt CJ, van Giersbergen PL, White HS, Siegel BW, Senyah Y, McCloskey TC, Fadayel GM, Taylor VL, Murawsky MK, Nyce P, Salituro FG (1997) Pharmacological characterization of MDL 105,519, an NMDA receptor glycine site antagonist. Eur J Pharmacol 323:181–192.

Berman RM, Cappiello A, Anand A, Oren DA, Heninger GR, Charney DS, Krystal JH (2000) Antidepressant effects of ketamine in depressed patients. Biol Psychiatry 47:351–354.

Burgdorf J, Kroes RA, Zhang XL, Gross AL, Schmidt M, Weiss C, Disterhoft JF, Burch RM, Stanton PK, Moskal JR (2015a) Rapastinel (GLYX-13) has therapeutic potential for the treatment of post-traumatic stress disorder: characterization of a NMDA receptor-mediated metaplasticity process in the medial prefrontal cortex of rats. Behav Brain Res 294:177–185.

Burgdorf J, Zhang XL, Nicholson KL, Balster RL, Leander JD, Stanton PK, Gross AL, Kroes RA, Moskal JR (2013) GLYX-13, a NMDA receptor glycine-site functional partial agonist, induces antidepressant-like effects without ketamine-like side effects. Neuropsychopharmacology 38:729–742.

Burgdorf J, Zhang XL, Weiss C, Gross A, Boikess SR, Kroes RA, Khan MA, Burch RM, Rex CS, Disterhoft JF, Stanton PK, Moskal JR (2015b) The long-lasting antidepressant effects of rapastinel (GLYX-13) are associated with a metaplasticity process in the medial prefrontal cortex and hippocampus. Neuroscience 308:202–211.

Erreger K, Geballe MT, Dravid SM, Snyder JP, Wyllie DJ, Traynelis SF (2005) Mechanism of partial agonism at NMDA receptors for a conformationally restricted glutamate analog. J Neurosci 25:7858–7866.

Gerhard DM, Wohleb ES, Duman RS (2016) Emerging treatment mechanisms for depression: focus on glutamate and synaptic plasticity. Drug Discov Today 21:454–464.

Izumi Y, Zorumski CF (2014) Metaplastic effects of subanesthetic ketamine on CA1 hippocampal function. Neuropharmacology 86:273–281.

Kehr J, Yoshitake T (2006) Monitoring brain chemical signals by microdialysis. In: Encyclopedia of sensors (Grimes CA, Dickey EC, Pishko MV, eds), pp 287–312. Valencia, CA: American Scientific Publishers.

Kehr J, Yoshitake T (2017) Derivatization chemistries for improved detection of monoamine neurotransmitters and their metabolites in microdialysis samples by liquid chromatography with fluorescence detection and mass spectrometry. In: Compendium of in-vivo monitoring in real-time molecular neuroscience, Vol. 2, microdialysis and sensing of neural tissues (Wilson G, Michael A, eds), pp 193–216. Singapore: World Scientific Publishing.

Kemp JA, Foster AC, Leeson PD, Priestley T, Tridgett R, Iversen LL, Woodruff GN (1988) 7-Chlorokynurenic acid is a selective antagonist at the glycine modulatory site of the N-methyl-D-aspartate receptor complex. Proc Natl Acad Sci U S A 85:6547–6550.

Koike H, Iijima M, Chaki S (2011) Involvement of AMPA receptor in both the rapid and sustained antidepressant-like effects of ketamine in animal models of depression. Behav Brain Res 224:107–111.

Li N, Lee B, Liu RJ, Banasr M, Dwyer JM, Iwata M, Li XY, Aghajanian G, Duman RS (2010) mTOR-dependent synapse formation underlies the rapid antidepressant effects of NMDA antagonists. Science 329:959–964.

Li N, Liu RJ, Dwyer JM, Banasr M, Lee B, Son H, Li XY, Aghajanian G, Duman RS (2011) Glutamate N-methyl-D-aspartate receptor antagonists rapidly reverse behavioral and synaptic deficits caused by chronic stress exposure. Biol Psychiatry 69:754–761.

Liu RJ, Duman C, Kato T, Hare B, Lopresto D, Bang E, Burgdorf J, Moskal J, Taylor J, Aghajanian G, Duman RS (2017) GLYX-13 produces rapid antidepressant responses with key synaptic and behavioral effects distinct from ketamine. Neuropsychopharmacology 42:1231–1242.

Liu RJ, Lee FS, Li XY, Bambico F, Duman RS, Aghajanian GK (2012) Brain-derived neurotrophic factor val66met allele impairs basal and ketamine-stimulated synaptogenesis in prefrontal cortex. Biol Psychiatry 71:996–1005.

Lorrain DS, Baccei CS, Bristow LJ, Anderson JJ, Varney MA (2003) Effects of ketamine and N-methyl-D-aspartate on glutamate and dopamine release in the rat prefrontal cortex: modulation by a group II selective metabotropic glutamate receptor agonist LY379268. Neuroscience 117:697–706.

Maeng S, Zarate CA Jr, Du J, Schloesser RJ, McCammon J, Chen G, Manji HK (2008) Cellular mechanisms underlying the antidepressant effects of ketamine: role of alpha-amino-3-hydroxy-5-methylisoxazole-4-propionic acid receptors. Biol Psychiatry 63:349–352.

Malenka RC, Bear MF (2004) LTP and LTD: an embarrassment of riches. Neuron 44:5–21.

Miller OH, Moran JT, Hall BJ (2016) Two cellular hypotheses explaining the initiation of ketamine's antidepressant actions: direct inhibition and disinhibition. Neuropharmacology 100:17–26.

Moghaddam B, Adams B, Verma A, Daly D (1997) Activation of glutamatergic neurotransmission by ketamine: a novel step in the pathway from NMDA receptor blockade to dopaminergic and cognitive disruptions associated with the prefrontal cortex. J Neurosci 17:2921–2927.

Monteggia LM, Zarate C Jr (2015) Antidepressant actions of ketamine: from molecular mechanisms to clinical practice. Curr Opin Neurobiol 30:139–143.

Moskal JR, Kuo AG, Weiss C, Wood PL, O'Connor Hanson A, Kelso S, Harris RB, Disterhoft JF (2005) GLYX-13: a monoclonal antibody-derived peptide that acts as an N-methyl-D-aspartate receptor modulator. Neuropharmacology 49:1077–1087.

Moskal JR, Burch R, Burgdorf JS, Kroes RA, Stanton PK, Disterhoft JF, Leander JD (2014) GLYX-13, an NMDA receptor glycine site functional partial agonist enhances cognition and produces antidepressant effects without the psychotomimetic side effects of NMDA receptor antagonists. Expert Opin Investig Drugs 23:243–254.

Niciu MJ, Henter ID, Luckenbaugh DA, Zarate CA Jr, Charney DS (2014) Glutamate receptor antagonists as fast-acting therapeutic alternatives for the treatment of depression: ketamine and other compounds. Annu Rev Pharmacol Toxicol 54:119–139.

Parent MA, Wang L, Su J, Netoff T, Yuan LL (2010) Identification of the hippocampal input to medial prefrontal cortex in vitro. Cereb Cortex 20:393–403.

Paxinos G, Watson C (2007) *The Rat Brain in Stereotaxic Coordinates*, 7th edition. Burlington, MA: Elsevier Inc.

Posternak MA, Zimmerman M (2005) Is there a delay in the antidepressant effect? A meta-analysis. J Clin Psychiatry 66:148–158.

Preskorn S, Macaluso M, Mehra DO, Zammit G, Moskal JR, Burch RM; GLYX-13 Clinical Study Group (2015) Randomized proof of concept trial of GLYX-13, an N-methyl-D-aspartate receptor glycine site partial agonist, in major depressive disorder nonresponsive to a previous antidepressant agent. J Psychiatr Pract 21:140–149.

Rajagopal L, Burgdorf JS, Moskal JR, Meltzer HY (2016) GLYX-13 (rapastinel) ameliorates subchronic phencyclidine- and ketamine-induced declarative memory deficits in mice. Behav Brain Res 299:105–110.

Rodriguez CI, Zwerling J, Kalanthroff E, Shen H, Filippou M, Jo B, Simpson HB, Burch RM, Moskal JR (2016) Effect of a novel NMDA receptor modulator, rapastinel (formerly GLYX-13), in OCD: proof of concept. Am J Psychiatry 173:1239–1241.

Sanacora G, Johnson MR, Khan A, Atkinson SD, Riesenberg RR, Schronen JP, Burke MA, Zajecka JM, Barra L, Su HL, Posener JA, Bui KH, Quirk MC, Piser TM, Mathew SJ, Pathak S (2017) Adjunctive lanicemine (AZD6765) in patients with major depressive disorder and history of inadequate response to antidepressants: a randomized, placebo-controlled study. Neuropsychopharmacology 42:844–853.

Sanacora G, Treccani G, Popoli M (2012) Towards a glutamate hypothesis of depression: an emerging frontier of neuropsychopharmacology for mood disorders. Neuropharmacology 62:63–77.

Skolnick P, Layer RT, Popik P, Nowak G, Paul IA, Trullas R (1996) Adaptation of N-methyl-D-aspartate (NMDA) receptors following antidepressant treatment: implications for the pharmacotherapy of depression. Pharmacopsychiatry 29:23–26.

Urwyler S, Floersheim P, Roy BL, Koller M (2009) Drug design, in vitro pharmacology, and structure-activity relationships of 3-acylamino-2-aminopropionic acid derivatives, a novel class of partial agonists at the glycine site on the N-methyl-D-aspartate (NMDA) receptor complex. J Med Chem 52:5093–5107.

Valentine GW, Mason GF, Gomez R, Fasula M, Watzl J, Pittman B, Krystal JH, Sanacora G (2011) The antidepressant effect of ketamine is not associated with changes in occipital amino acid neurotransmitter content as measured by [(1)H]-MRS. Psychiatry Res 191:122–127.

Vose LR, Stanton PK (2017) Synaptic plasticity, metaplasticity and depression. Curr Neuropharmacol 15:71–86.

Warden D, Rush AJ, Trivedi MH, Fava M, Wisniewski SR (2007) The STAR*D project results: a comprehensive review of findings. Curr Psychiatry Rep 9:449–459.

Widman AJ, McMahon LL (2018) Disinhibition of CA1 pyramidal cells by low-dose ketamine and other antagonists with rapid antidepressant efficacy. Proc Natl Acad Sci U S A 115:E3007–E3016.

Wiescholleck V, Manahan-Vaughan D (2013) Long-lasting changes in hippocampal synaptic plasticity and cognition in an animal model of NMDA receptor dysfunction in psychosis. Neuropharmacology 74:48–58.

Williams NR, Heifets BD, Blasey C, Sudheimer K, Pannu J, Pankow H, Hawkins J, Birnbaum J, Lyons DM, Rodriguez CI, Schatzberg AF (2018) Attenuation of antidepressant effects of ketamine by opioid receptor antagonism. Am J Psychiatry. Advance online publication. Retrieved 19 Oct 2018. doi: 10.1176/appi.ajp.2018.18020138.

Williams NR, Schatzberg AF (2016) NMDA antagonist treatment of depression. Curr Opin Neurobiol 36:112–117.

Wohleb ES, Gerhard D, Thomas A, Duman RS (2017) Molecular and cellular mechanisms of rapid-acting antidepressants ketamine and scopolamine. Curr Neuropharmacol 15:11–20.

Yang B, Zhang JC, Han M, Yao W, Yang C, Ren Q, Ma M, Chen QX, Hashimoto K (2016) Comparison of R-ketamine and rapastinel antidepressant effects in the social defeat stress model of depression. Psychopharmacology (Berl) 233:3647–3657.

Zanos P, Moaddel R, Morris PJ, Georgiou P, Fischell J, Elmer GI, Alkondon M, Yuan P, Pribut HJ, Singh NS, Dossou KS, Fang Y, Huang XP, Mayo CL, Wainer IW, Albuquerque EX, Thompson SM, Thomas CJ, Zarate CA Jr, Gould TD (2016) NMDAR inhibition-independent antidepressant actions of ketamine metabolites. Nature 533:481–486.

Zarate CA Jr, Singh JB, Quiroz JA, De Jesus G, Denicoff KK, Luckenbaugh DA, Manji HK, Charney DS (2006) A double-blind, placebo-controlled study of memantine in the treatment of major depression. Am J Psychiatry 163:153–155.

Zhang XL, Sullivan JA, Moskal JR, Stanton PK (2008) A NMDA receptor glycine site partial agonist, GLYX-13, simultaneously enhances LTP and reduces LTD at schaffer collateral-CA1 synapses in hippocampus. Neuropharmacology 55:1238–1250.